

Modeling the effects of pitch-angle scattering processes on the transport of solar energetic particles along the interplanetary magnetic field

N. Agueda^{a,*}, D. Lario^b, E.C. Roelof^b, B. Sanahuja^a

^a *Departament d'Astronomia i Meteorologia, Universitat de Barcelona, Martí i Franques 1, 08028 Barcelona, Spain*

^b *The Johns Hopkins University Applied Physics Laboratory, 11100 Johns Hopkins Road, Laurel, MD 20723-6099, USA*

Received 15 November 2004; received in revised form 13 April 2005; accepted 17 April 2005

Abstract

We present a Monte-Carlo technique to study the time-dependent transport of energetic particles in the interplanetary medium. We use the guiding center approximation between discrete finite pitch-angle scatterings to quantify the competing effects of focusing and pitch-angle scattering on energetic particles propagating along a Parker spiral magnetic field. We consider that the pitch-angle scattering process is produced by small-scale magnetic field irregularities frozen in the expanding solar wind. We also include the effects of both solar wind convection and adiabatic deceleration. We use a *joint* probability distribution $P(h, \mu') = p(h; \mu')q(\mu'; \mu)$ to describe both the distance traveled by the particle between two scattering processes and the change in the particle pitch-angle after a scattering process. Here, $p(h; \mu')$ is the *conditional* probability that the particle travels a distance h along the field line before the next scattering *if* it had a pitch-angle cosine μ' after the previous scattering, and $q(\mu'; \mu)$ is the *conditional* probability for the pitch-angle cosine μ' *if* the pitch-angle cosine was μ before the scattering. We consider several functional forms to describe the processes of pitch-angle scattering, such as an isotropic scattering without any memory of the initial particle's pitch-angle or processes in which the scattering result depends upon the initial particle's pitch-angle. The results of our simulations are pitch-angle distributions and time-intensity profiles that can be directly compared to spacecraft observations. Comparison of our simulations with near-relativistic (45–290 keV) electron events observed by the Electron, Proton and Alpha Monitor on board the Advanced Composition Explorer allows us to estimate both the time dependence of the injection of near-relativistic electrons into the interplanetary medium and the conditions for electron propagation along the interplanetary magnetic field.

© 2005 COSPAR. Published by Elsevier Ltd. All rights reserved.

Keywords: Solar energetic particles; Interplanetary particle transport; Solar flares

1. Introduction

The two main processes that determine the time-intensity profiles of the solar energetic particle (SEP) events observed by spacecraft are particle injection into

the interplanetary medium and particle transport along the interplanetary magnetic field (IMF) lines. In order to infer the characteristics of the particle injection processes (i.e., the processes of particle acceleration and particle release close to the Sun) simulations of the interplanetary particle transport are required. Particle propagation in the interplanetary medium has long been studied (e.g., Roelof, 1969; Toptygin, 1985; Ruffolo, 1995; Dröge, 2000; and references therein). In this paper, we consider that energetic particles propagate along the IMF lines undergoing both pitch-angle scattering

* Corresponding author. Tel.: +34 93 402 11 22; fax: +34 93 402 11 33.

E-mail addresses: nagueda@am.ub.es (N. Agueda), david.lario@jhuapl.edu (D. Lario), edmond.roelof@jhuapl.edu (E.C. Roelof), blai.sanahuja@ub.edu (B. Sanahuja).

due to small-scale magnetic inhomogeneities and adiabatic focusing due to the varying magnitude of the large-scale component of the IMF.

We apply a Monte-Carlo technique to simulate both the processes of pitch-angle scattering and adiabatic focusing. Unlike previous studies using Monte-Carlo techniques (e.g., Earl, 1994; Kocharov et al., 1998; Li et al., 2003; Lintunen and Vainio, 2004), we use conditional probability distribution functions to describe first the distance traveled by the particles between two consecutive scatterings (assuming an initial pitch-angle cosine), and then the change in pitch-angle cosine due to the scattering itself. The scattering process is thought to be due to small-scale irregularities in the field that are considered to be frozen in the solar wind (Parker, 1965). We will assume that the interaction between particles and such irregularities only changes the particle pitch-angle whereas the energy of the particle is conserved in the frame of reference comoving with the field irregularities (i.e., the solar wind frame).

In this study, we follow the guiding center of the particle in a frame corotating with the Sun, where the large-scale structure of the magnetic field is static. Since pitch-angle scattering occurs in the system comoving with the solar wind, we need to include the local solar wind frame comoving with the solar wind velocity at a given point. We will assume that particles are able to freely propagate along a static Parker spiral magnetic field between discrete finite pitch-angle scatterings. That allows us to properly include magnetic focusing and mirroring with pitch-angle scattering. Scattering in the local solar wind frame of reference and focusing in the fixed frame of reference leads to systematic decreases of the particle energy in the fixed reference frame as the particle moves away from the Sun (Ruffolo, 1995). In the following, z denotes the distance from the Sun along the magnetic field line and μ the pitch-angle cosine of the particle.

2. The model

Once the energetic particles escape from their source, they propagate along the ambient magnetic field, described by the Parker spiral. In this treatment, particles conserve their magnetic moment along the IMF and experience occasionally pitch-angle scattering by fluctuations in the magnetic field. We will assume that pitch-angle scattering is mainly due to interactions between particles and field fluctuations with wavelengths in resonance with the particle motion along the field. Thus, the amount of scattering a particle experiences basically depends on the power density of the waves at the resonance frequency. Therefore, the distance h that the particle travels along the field line between two consecutive scatterings may depend on $|\mu|$. We assume that h

is distributed according to an exponential probability distribution function for a Poisson process

$$p(h; \eta) = \frac{1}{\eta} e^{-h/\eta}, \quad (1)$$

where η (which may be a function of μ) depends on the details of the theoretical model for the pitch-angle cosine scattering process. We have simply chosen two ad hoc forms

$$\eta(\mu) = \lambda_{\parallel} \quad (2)$$

and

$$\eta(\mu) = -0.4|\mu| + \lambda, \quad (3)$$

where λ_{\parallel} and λ are free parameters, and λ_{\parallel} is the equivalent to the particle mean free path. The units of the distance h are determined by the units used in λ and λ_{\parallel} . It is easy to verify that $\int p(h; \eta) dh = 1$ for any choice of η . Eq. (2) assumes that h is not a function of the pitch-angle cosine, while Eq. (3) does. The use of Eq. (3) implies that particles with large pitch-angle (i.e., $\mu \sim 0$) may propagate a larger distance between two consecutive scatterings (hence a larger h), whereas particles with smaller pitch-angles ($|\mu| \sim 1$) may see more magnetic field irregularities along their travel between two consecutive scatterings (hence a smaller h). We define $\mu > 0$ to be outward from the Sun, therefore particles with $\mu < 0$ move back toward the Sun and may experience mirroring. On the other hand, particles with $\mu > 0$ will decrease their pitch-angle ($\mu \rightarrow 1$) as they move away from the Sun. For any given h , we can relate the initial and final positions between two consecutive scattering processes, z_i and z_f , through, $z_f = z_i + \text{sign}(\mu)h$, if the particle does not experience mirroring. In the other case, $z_f = z_m + h - (z_i - z_m)$, where z_m is the mirroring point.

Energetic particle pitch-angle scattering is caused by irregularities of the IMF that violate the conservation of the first adiabatic invariant (Dröge, 2000). The interaction between energetic particles and these magnetic irregularities entails a change in the pitch-angle cosine of the particle from μ to μ' . The pitch-angle cosine scattering process itself ($\mu \rightarrow \mu'$) is in general a function of the initial pitch-angle cosine μ . Approaches used to describe the pitch-angle scattering processes in a Monte-Carlo technique range from isotropic small-angle rotations of the initial particle velocity vector performed in small time steps during the particle transport (e.g., Lintunen and Vainio, 2004) to an isotropic and Markovian process in which the new pitch-angle is randomly chosen losing any memory of the initial pitch-angle (Li et al., 2003). In this paper, we perform a pitch-angle scattering every time a particle moves a distance h along the IMF line. The scattering centers are assumed to be frozen in the solar wind. Thus, prior to each scattering, the velocity vector of the particle is Lorentz transformed to the scattering-center frame; the scattering is performed con-

servicing the particle speed in this frame; and then, after scattering, the new velocity vector is transformed back to the fixed corotating frame where the particle moves a new step h according to its new parallel velocity.

We consider three different probability distribution functions that characterize the pitch-angle scattering process from a completely isotropic scattering to a small-angle interaction. We define $q(\mu'; \mu)$ as the conditional probability distribution function for the pitch-angle cosine μ' after the scattering in the solar wind frame, when the pitch-angle cosine before the interaction was μ , in the same reference frame. We consider the following three cases:

(1) *Gaussian*: We define $q(\mu'; \mu)$ by

$$q(\mu'; \mu) = \frac{1}{\sqrt{2\pi\sigma^2}} \frac{1}{1 - \mu'^2} e^{-(x' - x)^2 / 2\sigma^2}, \quad (4)$$

where

$$x' - x = \frac{1}{2} \ln \frac{(1 + \mu')(1 - \mu)}{(1 - \mu')(1 + \mu)}. \quad (5)$$

This function distributes the values of μ' around the initial pitch-angle cosine μ , in such a way that the scattering conserves most of the initial pitch-angle information. Thus, to turn a particle around, a large number of interactions are required. We may consider the parameter σ to be a function of the initial pitch-angle cosine μ . This is physically necessary in the presence of a mean magnetic field, because small-angle scattering is stronger (large σ) when $\mu \cong \pm 1$ and weaker (small σ) when $\mu \cong 0$. To avoid the δ -function nature of the probability distribution $q(\mu'; \mu)$ when $\mu \rightarrow \pm 1$, σ is chosen to depend on the pitch-angle cosine like $\sigma(\mu) = -\ln(1 - \mu^2) + \sigma_1$, where $\sigma_1 = 0.01$. The bottom panel of Fig. 1 shows

$q(\mu'; \mu)$ for different values of the initial pitch-angle cosine μ .

(2) *Uniform (or isotropic)*: The final pitch-angle cosine μ' is isotropically chosen between -1 and $+1$. This corresponds to a very efficient scattering process, because the result of the scattering has no memory of the initial pitch-angle.

(3) *Triangular*: We define $q(\mu'; \mu)$ by

$$q(\mu'; \mu) = \begin{cases} \frac{b-a}{\mu+1} \mu' + \frac{a\mu+b}{\mu+1} & \text{if } \mu' < \mu, \\ \frac{b-c}{\mu-1} \mu' + \frac{c\mu-b}{\mu-1} & \text{if } \mu' \geq \mu, \end{cases} \quad (6)$$

where a and c are parameters chosen to satisfy the conditions:

- when $\mu = 1$, $q(\mu'; \mu)$ is a uniform probability distribution function;
- when $\mu = 0$, $q(\mu'; \mu)$ is a symmetric triangular probability distribution function;
- the result of the pitch-angle scattering favors the direction of particle propagation before the scattering process, except the case with $|\mu| = 1$ where μ' is uniformly distributed.

The parameter b is then deduced by imposing that $\int q(\mu'; \mu) d\mu' = 1$. Taking $a = \mu^2/2$ and $c = \mu/2$, then $b = 1 - \mu^2/4(\mu^2 + 1)$ for $q(\mu'; \mu \geq 0)$ and $q(\mu'; \mu < 0) = q(-\mu'; \mu \geq 0)$. This distribution function is a mathematical intermediate case between the Uniform and Gaussian cases in the sense that the function peaks at $\mu' = \mu$, but when $\mu \rightarrow \pm 1$ the distribution function becomes uniform. This assumption implies that particles within $|\mu| \sim 1$ are more likely to undergo a large-angle interaction whereas particles with $|\mu| \sim 0$ are more likely to remain within a pitch-angle similar to the initial pitch-angle. The top panel of Fig. 1 shows the case of triangular $q(\mu'; \mu)$ for different values of the initial pitch-angle cosine μ .

The above conditional probability distribution functions $q(\mu'; \mu)$ represent three different mathematical parameterizations of the pitch-angle scattering processes. They are not based on a given physical model of the interaction between energetic particles and the underlying magnetic field irregularities. The cases 1 and 3 represent conditional probability distributions that have some “memory” of the pre-scattered pitch-angle cosine (μ) to sample the result of the interaction (μ'), whereas the case 2 does not retain any memory of the pitch-angle before the scattering process. While the case 2 acts uniformly over all initial pitch-angles, the cases 1 and 3 assume that the scattering process acts more efficiently on particles with small pitch-angles.

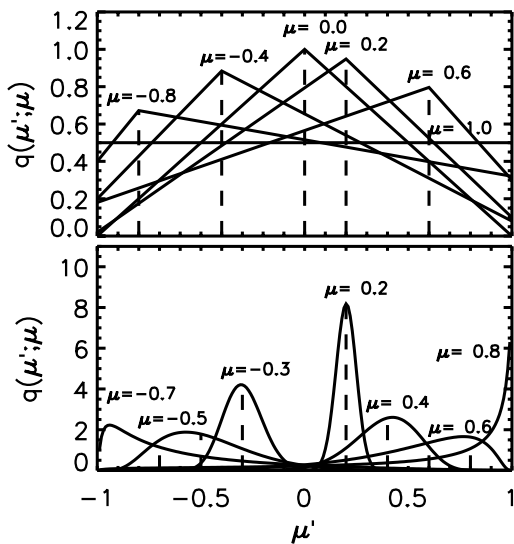


Fig. 1. Conditional probability distribution functions $q(\mu'; \mu)$ for different scattering processes and for different initial pitch-angles (μ): triangular scattering (top panel) and Gaussian scattering (bottom panel).

3. Parametric study

For a parametric study, we chose the case of 45–290 keV electrons isotropically injected in the outward

direction from the Sun at a radial distance 0.01 AU from the center of the Sun. We assume that the injection follows a time profile given by

$$Q(t) \propto \exp\left(\frac{-(t-t_0)^2}{\delta}\right), \quad (7)$$

where $t \geq 0$, and t_0 corresponds to the peak injection time and δ is the half-width of the Gaussian distribution. We also assume a power-law energy spectra, $E^{-\gamma}$, with spectral index $\gamma = 3$.

The method of registration involves the record of the energy and the pitch-angle cosine of the particles that cross the observer each time. This information allows us to compute the number of particles at the observer's location as a function of time, energy and direction (i.e., the differential flux). $\Delta\mu$ and Δt are the bin widths for the pitch-angle cosine and for the time, respectively, $\Delta\mu = 0.1$ and $\Delta t = 72$ s. For the registration of the energy, we take the energy bin widths that correspond to the energy channels of the LEFS60 telescope of the Electron, Proton and Alpha Monitor (EPAM) instrument on board the Advanced Composition Explorer (ACE) spacecraft (Gold et al., 1998). We can then compute: (1) pitch-angle distributions (PADs) as a function of time and energy; (2) time-intensity profiles observed during an event; (3) mean pitch-angle cosine $\langle\mu\rangle$ as a function of time and energy (when we integrate over all directions).

Fig. 2 shows the omni-directional-averaged time profiles of the 45–62 keV electron intensity (top panels) and of $\langle\mu\rangle$ (bottom panels) as measured by an observer at a radial distance of 1 AU. The common line shown in Fig. 2(a–c) (solid line) is the result of assuming an injection given by Eq. (7) (with $\delta = 15$ min and $t_0 = 30$ min) at

0.01 AU, uniform scattering (case 2 in Section 2) and $\eta(\mu)$ given by Eq. (3) with $\lambda = 1$ AU. Fig. 2(a) shows the dependence of the time-intensity and $\langle\mu\rangle$ profiles on the different values of λ . The larger the λ , the faster the intensity increase to a maximum, the earlier the maximum of intensity and the higher the values of $\langle\mu\rangle$ through the rising and maximum phase of the event. For values of λ greater than the observer radial distance (i.e., $\lambda \geq 1$ AU), the influence of the interplanetary scattering on the onset phase of the event is almost negligible. Particles reaching 1 AU at early times correspond to particles that propagated scatter-free. Indeed, according to Eq. (1), even for small values of λ , there is still a small population of particles that can cross 1 AU without having undergone any significant pitch-angle scattering process. Therefore, the simulation computes the same onset in all the three cases. Fig. 2(a) also shows that the initial value of $\langle\mu\rangle$ is close to 1 for all cases, corresponding to particles that propagated nearly scatter-free and focused along the IMF line. At later times, smaller values of λ (compared with $\lambda = 1$ AU) produce smaller values of $\langle\mu\rangle$ as a result of the higher number of pitch-angle scatterings.

Fig. 2(b) shows the dependence of the time-intensity and $\langle\mu\rangle$ profiles on the function $q(\mu'; \mu)$. The nature of the scattering process notably plays an important role in the decay phase of the event. Since Gaussian scattering (case 1 in Section 2) strongly preserves the initial pitch-angle, $\langle\mu\rangle$ values stay longer close to 1, and the decay phase of the event is shorter and faster. On the other hand, the uniform scattering (case 2 in Section 2) produces drastic changes in μ after each scattering process, and hence, the smaller values of $\langle\mu\rangle$ and the longer and slower decay of the intensities.

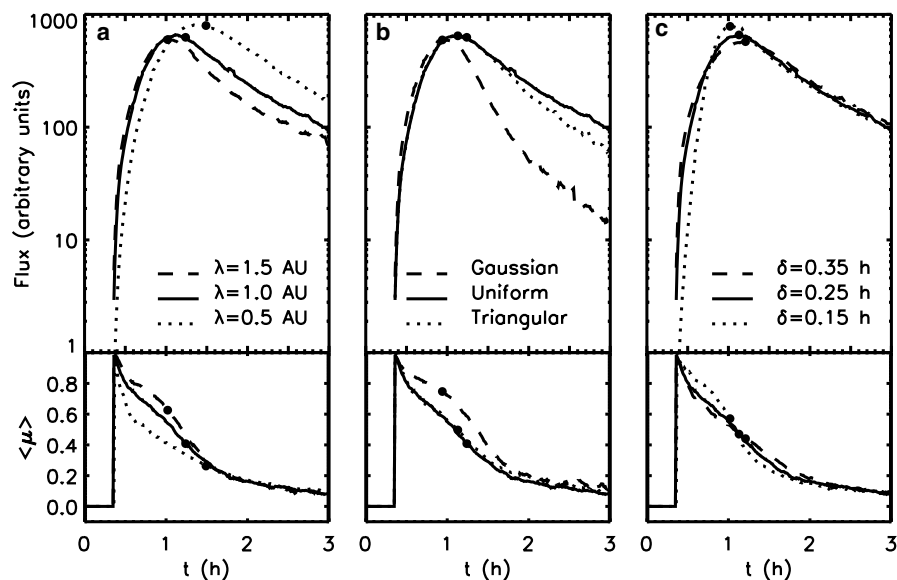


Fig. 2. 45–62 keV electron intensity-time profiles obtained by the model for: (a) different values of λ ; (b) different types of scattering processes; (c) different injection profiles at the source.

Finally, Fig. 2(c) shows the dependence on the particle injection, specifically on the injection parameter δ . The time-intensity profile during the onset phase is clearly dominated by the source injection with faster rises to maximum intensity for smaller values of δ . However, the injection does not play a significant role in the decay phase if it is short-lived.

4. Application of the model

We have applied the model to the impulsive electron event observed by the LEFS60 telescope of ACE/EPAM (Gold et al., 1998) on 2000 May 1. According to Kahler et al. (2001) the origin of this event was associated with a narrow fast CME propagating away from the west limb of the Sun first seen above 2 solar radii at 10:54 UT on 2000 May 1 and an M1.1 X-ray solar flare from approximately N20W54. The 1–8 Å X-ray emission lasted from 10:16 to 10:34 UT, peaking at 10:27 UT. The SEP event was classified as impulsive not only because of its high Fe/O and $^3\text{He}/^4\text{He}$ ratios (Mason et al., 2002) and low H/He ratios (Kahler et al., 2001), but also because of its short duration and extremely anisotropic onset (Ho et al., 2003). Fig. 3 shows the 175–290 keV electron spin-averaged intensity-time profile observed by ACE/EPAM/LEFS60 (solid line) and the profile calculated

by the model (dashed line), assuming a uniform scattering (case 2 in Section 2) and $\lambda_{||} = 2.7$ AU in Eq. (2). The assumed Gaussian injection profile, scaled with energy as E^{-3} , starts at 10:16 UT and lasts 17 min (dotted line in Fig. 3).

With this set of parameters we have been able to fit an envelope to the spin-averaged intensity history. The computed intensity matches the rise to maximum and initial decay down to about a factor of 3 below the peak. At that point (10:40 UT), the measured intensity continues its rapid decline, while the computed spin-averaged intensity diverges with a steadily decreasing rate of decay that joins the final decay phase of the measured intensity at about 10:50 UT. The measured intensities begin their gradual decay only after rising from their local minimum at 10:45 UT.

Fig. 4 shows the 175–290 keV electron PADs averaged over 72 s as observed by the LEFS60 telescope. This telescope consists of eight sectors (numbered from 1 to 8 in Fig. 4). The PADs plotted in Fig. 4 assign a single pitch-angle value to each sector (considered to be the angle between the instantaneous magnetic field vector and the direction of the center of the sector). Therefore, the corresponding intensity represents an integration over the range of pitch-angle scanned by the telescope during the spin time of each sector. The dashed lines

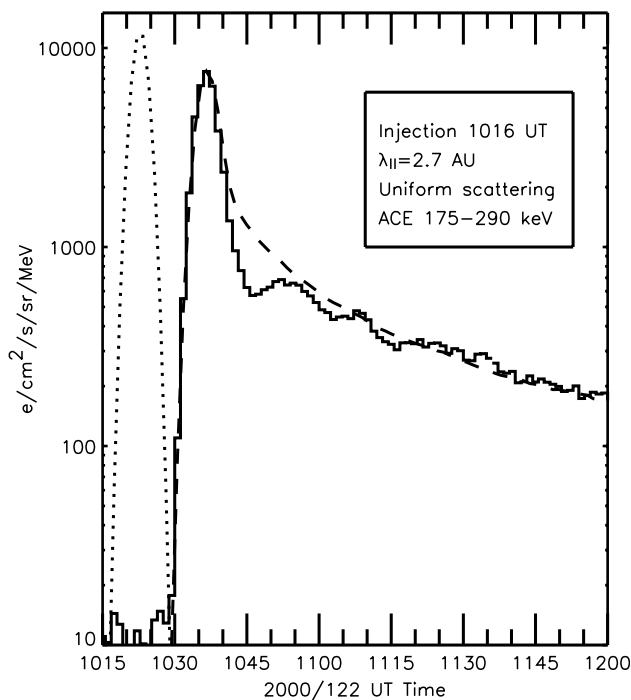


Fig. 3. 175–290 keV electron intensity-time profile observed on 2000 May 1 at 1 AU by the LEFS60 telescope of the EPAM instrument on board ACE (solid line) and time-intensity profiles as computed by the model (dashed line). Temporal injection profile of energetic electrons at the source is represented (dotted line).

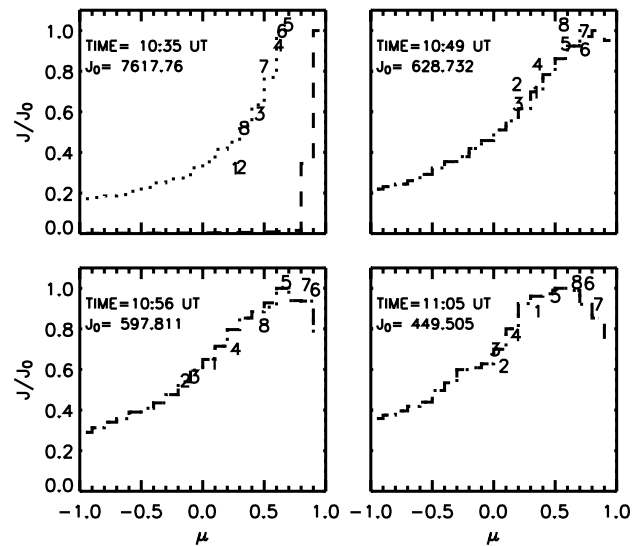


Fig. 4. Seventy-two seconds averaged 175–290 keV electron pitch-angle distributions observed by the LEFS60 telescope of the EPAM instrument on board ACE and values obtained by the model. Each number (1–8) gives the intensity observed in each one of the eight sectors of the LEFS60 telescope normalized to the sector with maximum intensity (J_0). The units of J_0 are in $(\text{cm}^2 \text{ s sr MeV})^{-1}$. Dashed lines show modeled PADs, obtained by sorting the electron data into $\Delta\mu = 0.1$ bins and normalized to the bin with maximum intensity. The dotted line in the first panel shows the normalization of the simulated PADs with the largest observed pitch-angle cosine scanned by the LEFS60 telescope. In the other three panels the dotted line essentially coincides with the corresponding dashed line.

show the PADs derived by the model. Early in the event, the simulated PADs are focused around $\mu = 1$. At that time, the orientation of the LEFS60 telescope and the direction of the IMF were such that the largest pitch-angle cosine scanned by the instrument was only ~ 0.7 . Normalization of the simulated PADs to the flux observed with the largest observed pitch-angles (dotted line in Fig. 4) compares well with the observations. Later in the event, after $\sim 10:49$ UT, model and observations agree in both intensity and PADs and the intensity of particles with $\mu < 0$ predicted by the model gradually increases.

The discrepancy between model and observations at the time of the local minimum of the observed intensities (between 10:40 and 10:50 UT) suggests an alternative scenario for this event. The electrons seen by ACE between 10:29 and 10:45 UT (first hump in the spin-averaged intensity in Fig. 3) may result from an extended solar injection and scatter-free propagation between the Sun and the spacecraft, whereas the gradual decay in the spin-averaged intensity (after 10:50 UT) results from back-scatter processes occurring beyond 1 AU. Intensities observed during this long-decay are formed by those electrons reflected back from beyond 1 AU moving sunward and those electrons that move anti-sunward after mirroring at some inner heliocentric distance as a consequence of the converging magnetic field close to the Sun. The distance where these particles mirror depends on their initial pitch-angle as they move back toward the Sun. The result of both processes is the gradual decay of intensities observed at 1 AU and the slow filling of the $\mu < 0$ hemisphere of the PADs. Simulation considering back-scatter processes from local magnetic field enhancements beyond 1 AU will be incorporated in future works.

5. Conclusions

We have developed a Monte-Carlo technique to study the time-dependent transport of energetic particles in the interplanetary medium. Once energetic electrons escape from their source, we assume that their subsequent motion is along the ambient magnetic field, described by a Parker spiral. In this treatment, the guiding-center of the particle simply moves along the IMF while the particle occasionally experiences pitch-angle scattering by fluctuations in the magnetic field. We use a *joint* probability distribution $P(h, \mu') = p(h; \mu')q(\mu'; \mu)$. Here, $p(h; \mu')$ is the conditional probability that the particle travels a distance h along the field line before the next scattering if it had a pitch-angle cosine μ' after the previous scattering, and $q(\mu'; \mu)$ is the conditional probability for the post-scattered pitch-angle cosine μ' given that the pre-scattered pitch-angle cosine was μ before the previous scattering. We have

assumed several functional forms for $p(h; \mu')$ and $q(\mu'; \mu)$.

The model developed has allowed us to study the characteristics of the time-intensity and time- $\langle \mu \rangle$ profiles at 1 AU, as well as the pitch-angle distributions. In particular, we have studied the dependence of the profiles on the functions $p(h; \mu')$ and $q(\mu'; \mu)$, as well as on the source injection time-profile.

To check the outputs of this code we have studied an energetic electron event observed on 2000 May 1 by ACE/EPAM. A Gaussian finite-duration solar injection starting at 10:16 UT and lasting 17 min, a mean free path of 2.7 AU and an isotropic pitch-angle scattering process, allows us to fit the 175–290 keV electron flux observed during the rising phase of the event, including the peak intensity and its initial decay. The adopted value for the mean free path ($\lambda_{\parallel} = 2.7$ AU in Eq. (2)) represents a nearly scatter-free propagation that fails to reproduce the rapid intensity decay observed after the first hump at 10:45 UT. The value considered for the mean free path in this specific event should be understood in the context of the simulation performed in this paper and the functions $p(h; \mu')$ and $q(\mu'; \mu)$ chosen to model it. The intensity and PADs observed during this impulsive electron event show that the degree of pitch-angle scattering undergone by these particles should be very small and much lower than those derived from the values of λ_{\parallel} that have appeared over the years in the literature (e.g., Dröge, 2000, and references therein).

Acknowledgments

The work at DAM/UB was supported by the Spanish Ministerio de Educacion y Ciencia (MEC) under Project AYA2001-3304 and Grant BES-2002-0026. The work at JHU/APL was partially supported by NASA under Grant NAG5-10787. N.A. acknowledges the support of ESA Education Department for the student participation on the 35th COSPAR Scientific Assembly. N.A. thank Josep Sempau (INTE/UPC) for valuable discussions and helpful comments regarding this work.

References

- Dröge, W. The rigidity dependence of solar particle scattering mean free paths. *Astrophys. J.* 537, 1073–1079, 2000.
- Earl, J.A. New description of charged particle propagation in random magnetic fields. *Astrophys. J.* 425, 331–342, 1994.
- Gold, R.E., Krimigis, S.M., Hawkins III., S.E., et al. Electron, proton, and alpha monitor on the advanced composition explorer spacecraft. *Space Sci. Rev.* 86, 541–562, 1998.
- Ho, G.C., Roelof, E.C., Mason, G.M., et al. Onset study of impulsive solar energetic particle events. *Adv. Space Res.* 32, 2679–2684, 2003.

- Kahler, S.W., Reames, D.V., Sheeley Jr., N.R. Coronal mass ejections associated with impulsive solar energetic particle events. *Astrophys. J.* 562, 558–565, 2001.
- Kocharov, L., Vainio, R., Kovaltsov, G.A., et al. Adiabatic deceleration of solar energetic particles as deduced from Monte Carlo simulations of interplanetary transport. *Solar Phys.* 182, 195–215, 1998.
- Li, G., Zank, G.P., Rice, W.K.M. Energetic particle acceleration and transport at coronal mass ejection-driven shocks. *J. Geophys. Res.* 108, A2, 2003, doi:10.1029/2002JA009666.
- Lintunen, J., Vainio, R. Solar energetic particle event onset as analyzed from simulated data. *Astron. Astrophys.* 420, 343–350, 2004.
- Mason, G.M., Wiedenbeck, M.E., Miller, J.A., et al. Spectral properties of He and heavy ions in ³He-rich solar flares. *Astrophys. J.* 574, 1039–1058, 2002.
- Parker, E.N. The passage of energetic charged particles through interplanetary space. *Planet. Space Sci.* 13, 9–49, 1965.
- Roelof, E.C. Propagation of Solar Cosmic Rays in the Interplanetary Magnetic Field. Lectures in High-Energy Astrophysics, NASA SP-199. Scientific and Technical Information Division, Office of Technology Utilization, NASA, Washington, p. 111, 1969.
- Ruffolo, D. Effect of adiabatic deceleration on the focused transport of solar cosmic rays. *Astrophys. J.* 442, 861–874, 1995.
- Toptygin, I.N. Cosmic Rays in Interplanetary Magnetic Fields. D. Reidel Publishing Co., Dordrecht, p. 375, 1985.